Acknowledgements

We thank R. M. Zinkernagel, F. Melchers and J. E. DeVries for critically reviewing the manuscript, as well as C. H. Heusser and S. Alkan for anti-IL-4 and anti-IFN-γ antibodies. This work was sponsored by the Swiss National Science Foundation.

Correspondence and requests for materials should be addressed to M.J. (e-mail: marek.jutel@siaf.unizh.ch) or C.A.A. (e-mail: akdisac@siaf.unizh.ch).

Auxin transport inhibitors block PIN1 cycling and vesicle trafficking

Niko Geldner*†, Jiří Friml†‡§‖, York-Dieter Stierhof*, Gerd Jürgens* & Klaus Palme‡

** Zentrum für Molekularbiologie der Pflanzen, Universität Tübingen, Auf der Morgenstelle 3, D-72076 Tübingen, Germany*
‡ Max-Delbrück-Laboratorium in der Max-Planck-Gesellschaft, D-50829 Köln, Germany
§ Department of Biochemistry, Faculty of Science, Masaryk University, Kotlářská 2, 61137 Brno, Czech Republic
† These authors contributed equally to this work

Polar transport of the phytohormone auxin mediates various processes in plant growth and development, such as apical dominance, tropisms, vascular patterning and axis formation[1,2]. This view is based largely on the effects of polar auxin transport inhibitors. These compounds disrupt auxin efflux from the cell but their mode of action is unknown[3]. It is thought that polar auxin flux is caused by the asymmetric distribution of efflux carriers acting at the plasma membrane[4]. The polar localization of efflux carrier candidate PIN1 supports this model[4]. Here we show that the seemingly static localization of PIN1 results from rapid actin-dependent cycling between the plasma membrane and endosomal compartments. Auxin transport inhibitors block PIN1 cycling and inhibit trafficking of membrane proteins that are unrelated to auxin transport. Our data suggest that PIN1 cycling is of central importance for auxin transport and that auxin transport inhibitors affect efflux by generally interfering with membrane-trafficking processes. In support of our conclusion, the vesicle-trafficking inhibitor brefeldin A mimics physiological effects of auxin transport inhibitors.

Polar auxin transport inhibitors are important tools in assessing the role of polar auxin transport in plant development[5–7]. They disrupt auxin efflux from the cell without interacting with the efflux carrier itself [8,9]. However, their mechanism of action has remained elusive despite considerable efforts towards the biochemical characterization of binding sites[10–12] and several screens for auxin-transport-inhibitor mutants[13–16]. *In situ* visualization of *Arabidopsis* putative auxin efflux carriers PIN1 and PIN2 correlated polar auxin transport with their asymmetric distribution in the plasma membrane[17,18]. This coordinated polar localization of PIN1 is not established in *gnom* mutant embryos. *GNOM* encodes a brefeldin A (BFA)-sensitive regulator of vesicle trafficking[19]. Consistent with this, the vesicle-trafficking inhibitor BFA affects auxin efflux from the cell[8,9], abolishes polar localization of PIN1 and induces its intracellular accumulation[19].

BFA-induced PIN1 accumulation in two large intracellular compartments was completely and rapidly reversible (Fig. 1a–c). To determine whether this reversible BFA effect reflects protein synthesis and degradation or continuous cycling between the plasma membrane and endosomal compartments, we inhibited protein synthesis by cycloheximide (CHX). Incubation of roots in 50 μM CHX for 30 min reduced ^{35}S-labelled methionine incorporation into proteins to below 10% of the control value (data not shown). However, treatment with 50 μM CHX for 4 h had no detectable effect on the amount of labelled PIN1 at the plasma membrane (Fig. 1d), suggesting that PIN1 protein is turned over slowly. CHX did not interfere with the reversible BFA effect as PIN1 still accumulated in endomembrane compartments (Fig. 1e) and, on withdrawal of BFA, reappeared at the plasma membrane (Fig. 1f). Thus, BFA-induced intracellular accumulation of PIN1 resulted from blocking exocytosis of a steady-state pool of PIN1 that rapidly cycles between the plasma membrane and some endosomal compartment.

In animal cells, BFA alters structure and function of endomembrane compartments, especially the Golgi apparatus, which fuses with other endomembranes[20–22]. BFA seems to have different effects in plant cells. In BFA-treated maize root cells, Golgi stack systems progressively disappear and aggregates of vesicles accumulate in their vicinity, with Golgi markers localizing to the newly formed

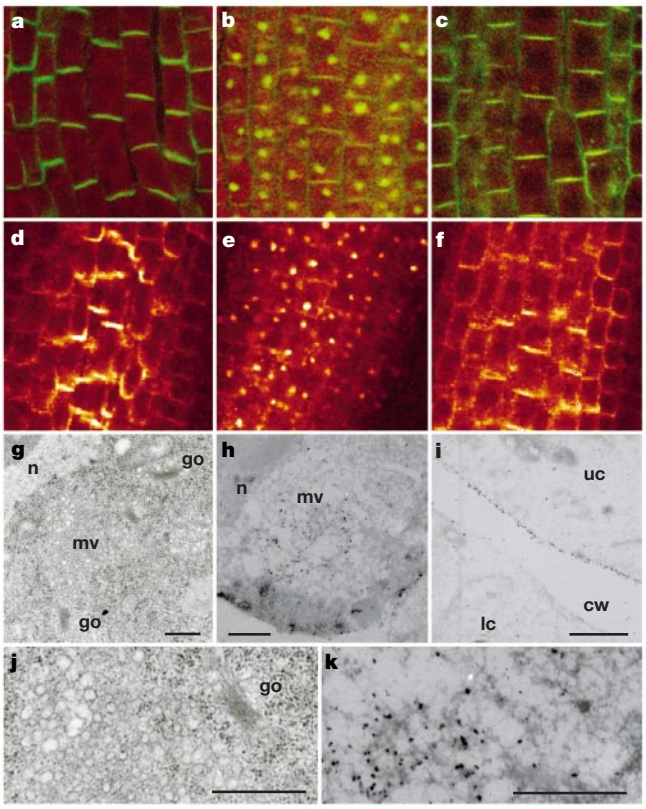

Figure 1 Reversible inhibition of PIN1 recycling by BFA treatment. **a**–**f**, *Arabidopsis* seedling roots treated with BFA or cycloheximide (CHX) as indicated. **a**, Two-hour buffer control. **b**, Treatment with 50 μM BFA for 2 h. **c**, Treatment with 50 μM BFA for 2 h followed by 2 h washing out. **d**, Treatment with 50 μM CHX for 2 h. **e**, Pre-treatment with 50 μM CHX for 30 min, then 50 μM BFA and 50 μM CHX for 90 min. **f**, Treatment with 50 μM BFA for 90 min, then 50 μM BFA and 50 μM CHX for 30 min followed by 2 h washing out with 50 μM CHX. **g**–**k**, Electron micrographs of root cells after treatment with 50 μM BFA for 30 min (**g**, **h**) and untreated control (**i**). **g**, Ultrastructure. **h**, **i**, Anti-PIN1 immunogold labelling. Note aggregate of membrane vesicles (mv) in ribosome-free cytoplasm near nucleus (n) and Golgi structures (go) of treated cells (**g**, **h**). **i**, Untreated control. Note PIN1 label at the plasma membrane of the upper cell (uc) but not the lower cell (lc). cw, cell wall. **j**, Higher magnification of **g**. **k**, Higher magnification of **h**. Scale bars, 1 μM.

‖ Present address: Zentrum für Molekularbiologie der Pflanzen, Universität Tübingen, Auf der Morgenstelle 3, D-72076 Tübingen, Germany.

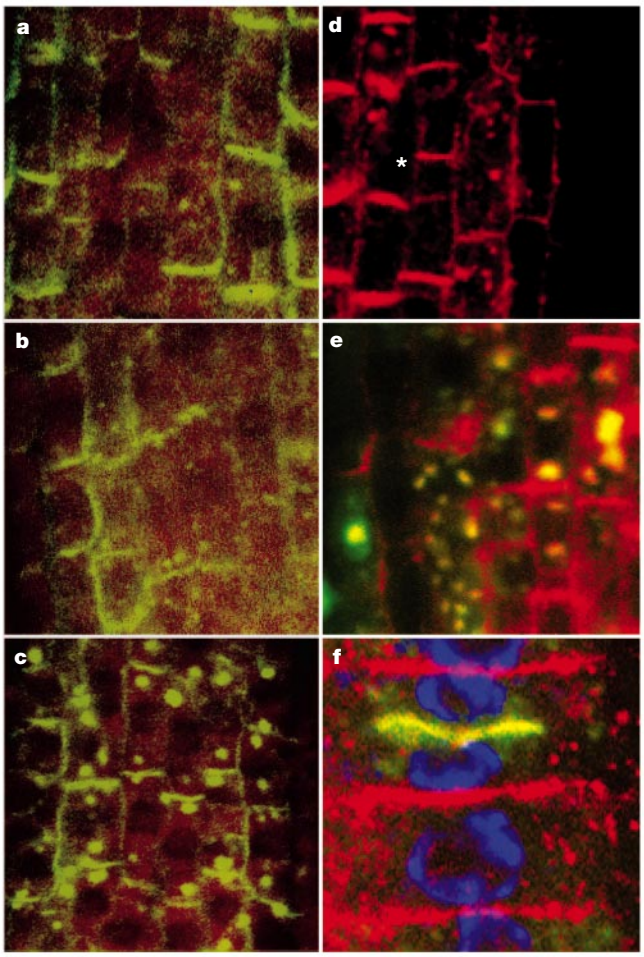

Figure 2 PIN1 localization affected by cytoskeleton-depolymerizing drugs. **a**–**c**, Cytochalasin D (cytD) effect on BFA inhibition of PIN1 (green) cycling. **a**, Treatment with 20 μM cytD for 2 h. **b**, Pre-treatment with 20 μM cytD for 15 min, then 50 μM BFA and 20 μM CytD for 45 min. **c**, Treatment with 50 μM BFA for 45 min followed by 90 min washing out BFA with 20 μM CytD. **d**, PIN1 staining after 10 μM oryzalin for 2 h—note patches in cell marked with asterisk as compared with normal localization in cell below. **e**, **f**, Colocalization of PIN1 (red) and KNOLLE (green) in small patches (yellow) after treatment with 10 μM oryzalin for 2 h (**e**), and in plane of cell division (yellow) of untreated control (**f**). DAPI staining of nuclei is blue.

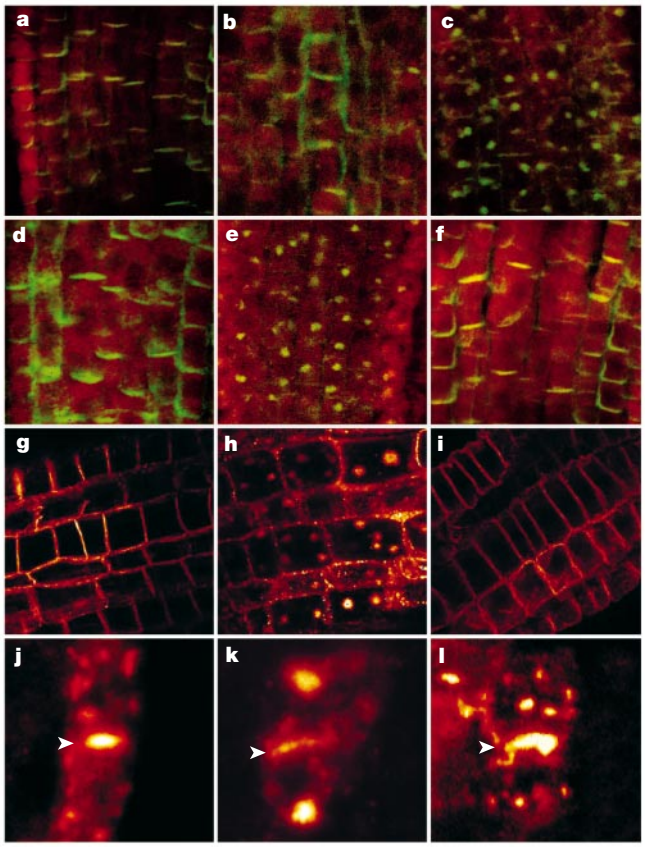

Figure 3 Effects of polar auxin transport inhibitor TIBA on protein trafficking. **a**–**f**, PIN1. **a**, Treatment with 25 μM TIBA for 2 h. **b**, Pre-treatment with 25 μM TIBA for 30 min, then 50 μM BFA and 25 μM TIBA for 2 h. **c**, Treatment with 50 μM BFA for 2 h followed by 2 h washing out of BFA with 25 μM TIBA. **d**, Treatment with 50 μM benzoic acid for 2 h (compare with **a**). **e**, Pre-treatment with 50 μM benzoic acid for 30 min, then 50 μM BFA and 50 μM benzoic acid for 2 h (compare with **b**). **f**, Treatment with 50 μM BFA for 2 h followed by 2 h washing out of BFA with 50 μM benzoic acid (compare with **c**). Note that BFA inhibition of PIN1 cycling was blocked only by TIBA but not by benzoic acid, which has no inhibitory activity on auxin transport. **g**–**i**, PM-ATPase. **g**, Untreated control. **h**, Treatment with 50 μM BFA for 90 min. **i**, Pre-treatment with 50 μM TIBA for 30 min, then 50 μM BFA and 50 μM TIBA for 90 min. **j**–**l**, KNOLLE. **j**, Untreated control. **k**, Treatment with 50 μM BFA for 2 h. **l**, Pre-treatment with 50 μM TIBA for 30 min, then 50 μM BFA and 50 μM TIBA for 2 h. Arrowheads mark cell plates. Note aggregation of KNOLLE label in large patches in **k** as compared with **j** and **l**.

BFA compartments[23,24]. In *Arabidopsis* root cells, the BFA-induced PIN1-labelled compartments were juxtanuclear, of a specific size and shape, and mostly two per cell (Fig. 1b). By electron microscopy, we identified aggregates of membrane vesicles of the corresponding size and shape that appeared only after BFA treatment (Fig. 1g, j). The vesicle aggregates were apparent within 30 min of BFA treatment, conditions that left individual Golgi stacks almost intact (Fig. 1g, j). These vesicle aggregates contained PIN1 protein that was apparently internalized from the plasma membrane (Fig. 1h, i, k). This result suggests that BFA compartments consist of vesicle aggregates that derive not only from Golgi stacks, as shown previously[23,24], but also from an as yet unidentified endosomal compartment.

The trafficking of membrane vesicles to sites of delivery takes place along the cytoskeleton[21,22]. To determine cytoskeletal requirements of PIN1 localization, we treated seedling roots with cytochalasin D (cytD) or latrunculin B, which both depolymerize actin filaments[25,26], or with oryzalin, which depolymerizes microtubules[25]. Cytochalasin D alone had only a slight effect on PIN1 polar accumulation at the plasma membrane, which was reduced, with small irregular dots of PIN1 label sometimes appearing underneath the plasma membrane (Fig. 2a). By contrast, cytD inhibited BFA-induced intracellular PIN1 accumulation (Fig. 2b) as well as its relocalization to the plasma membrane when BFA was washed out (Fig. 2c; compare with Fig. 1b, c). Latrunculin B had the same effects (data not shown). These results suggest that PIN1 cycling is actin dependent. By contrast, oryzalin treatment for up to 6 h did not alter PIN1 localization (Fig. 2d) nor internalization in response to BFA (data not shown), although the microtubules were completely depolymerized (data not shown). However, oryzalin treatment caused irregular patches of labelled PIN1 in some cells (Fig. 2d) that were shown to always coexpress the cytokinesis-specific syntaxin KNOLLE (Fig. 2e), which localizes to Golgi stacks and cell plate[27,28]. PIN1 and KNOLLE colocalized in oryzalin-treated cells (Fig. 2e), and both proteins were also detected at the cell plate of untreated cells (Fig. 2f). Thus, PIN1 seems to traffic along two different pathways, depending on the phase of the cell cycle: an actin-dependent interphase pathway to and from the plasma membrane and a microtubule-dependent cytokinesis pathway to the cell plate. PIN1 accumulation at the newly formed cell plate

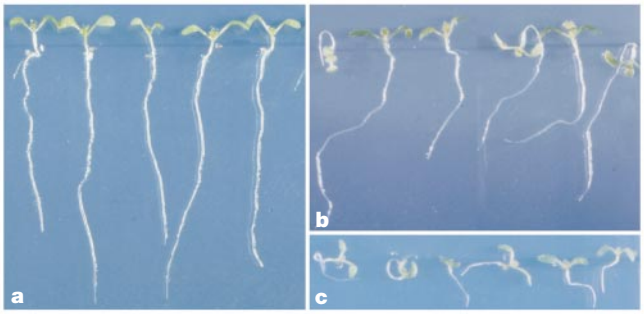

Figure 4 Physiological effects of BFA. Seedlings germinated on vertical agar plates containing different concentrations of BFA. **a**, Untreated control. **b**, Treatment with 10 μM BFA. **c**, Treatment with 20 μM BFA. Note the effect on gravitropic root growth and root elongation in **b** and **c**.

raises the question of how the coordinated polar localization of PIN1 is re-established after cell division, as only one of the two daughter cells would accumulate PIN1 at the correct end. The other daughter cell would initially have PIN1 localized at both ends, necessitating withdrawal of PIN1 from one end to reconstitute the original polarity of the cell.

Polar auxin transport inhibitors, such as 2,3,5-triiodobenzoic acid (TIBA), had only slight effects on PIN1 localization on their own (Fig. 3a). However, clear-cut effects were observed in BFA-treated cells. When cells were pre- and co-treated with TIBA, BFA did not induce intracellular accumulation of PIN1, which instead remained at the plasma membrane (Fig. 3b). Conversely, PIN1 remained at an intracellular position when BFA was washed out in the presence of TIBA (Fig. 3c). By contrast, an inactive analogue of TIBA, benzoic acid, did not interfere with the BFA-induced reversible internalization of PIN1 (Fig. 3d–f). Thus, BFA treatment revealed that polar auxin transport inhibitors block both the removal of PIN1 from and its redistribution to the plasma membrane.

To determine whether polar auxin transport inhibitors affect PIN1 cycling specifically, we analysed their effects on the localization of other membrane proteins whose trafficking was sensitive to BFA. Plasma membrane H^+-ATPase (PM-ATPase) is turned over rapidly at the plasma membrane[29]. Indeed, BFA treatment led to reversible intracellular accumulation of PM-ATPase in epidermal cells just above the cell division zone of the root tip. The BFA-induced intracellular compartments of PM-ATPase accumulation were similar in size and shape to those that accumulated PIN1 (Fig. 3g, h). In the presence of TIBA, BFA did not induce intracellular accumulation of PM-ATPase (Fig. 3i). Furthermore, recovery from the effect of BFA was blocked by washing with TIBA (data not shown). Thus, PM-ATPase trafficking was sensitive to polar auxin transport inhibitors, as was PIN1 trafficking. We also tested KNOLLE syntaxin[27]. With BFA treatment, small dots of labelled KNOLLE aggregated into larger patches (Fig. 3j, k). This BFA effect was also abolished by co-treatment with TIBA (Fig. 3l). Every polar auxin transport inhibitor that we tested had similar effects on the localization of all three proteins (PIN1, KNOLLE and PM-ATPase), although the effective concentrations were different, with 25 μM TIBA or 1-pyrenoylbenzoic acid (PBA) leading to complete inhibition of BFA-visualized trafficking, as compared with approximately 200 μM for 9-hydroxyfluorene-9-carboxylic acid (HFCA) or 1-*N*-naphthylphtalamic acid (NPA). Thus, a common feature of auxin-transport-inhibitor action seems to be a rather general influence on protein trafficking. We therefore tested whether the well established vesicle-trafficking inhibitor BFA might mimic physiological effects of auxin transport inhibitors. *Arabidopsis* seedlings were grown on vertical agar plates supplemented with low concentrations of BFA (Fig. 4). Several processes known to be sensitive to auxin transport inhibitors, such as root and hypocotyl gravitropism and elongation as well as lateral root initiation, were affected by BFA in a concentration-dependent manner (Fig. 4; Table 1). It is conceivable that compounds that were originally identified as polar auxin transport inhibitors may actually be inhibitors of membrane trafficking.

Our observations indicate that the putative auxin-efflux carrier PIN1 cycles between the plasma membrane and endosomal compartments in an actin-dependent manner. Auxin transport inhibitors block PIN1 cycling but, unlike BFA, leave PIN1 accumulation at the plasma membrane unaffected. This implies that cycling of some component of the auxin efflux machinery is essential for the mechanism of polar auxin transport. Notably, polar auxin transport inhibitors seem to interfere with membrane trafficking in broader terms, suggesting that their seemingly specific physiological effects may reflect a high sensitivity of auxin efflux carrier cycling and the important role of polar auxin flow in plant growth and development. □

Table 1 Quantitative effects of different BFA concentrations

	Concentration of BFA			
Area affected	0 μM	1 μM	10 μM	20 μM
Number of lateral roots	3.05 ± 1.21	3.48 ± 0.94	0.35 ± 0.49	0.10 ± 0.31
Root length (mm)	39.87 ± 3.66	37.70 ± 5.12	23.47 ± 4.91	7.07 ± 1.79
Hypocotyl length (mm)	23.1 ± 2.2	22.2 ± 2.4	18.6 ± 2.0	9.9 ± 2.7

Methods

Plant material and growth conditions

We grew *Arabidopsis* seedlings (Columbia ecotype) on vertical agar plates at 25 °C for 7 days.

Inhibitor treatments

Ten–fifteen seedlings were incubated in 1 ml liquid growth medium (0.5×MS medium, 0.8% sucrose, pH 5.8) containing the respective inhibitors or equal amounts of solvents (controls) in 24-well cell-culture plates. Washing was done twice for 10 min and a third washing step was carried out up to the indicated time. Incubations were stopped by fixation. BFA (Molecular Probes), TIBA (Duchefa), NPA (Duchefa), HFCA (Sigma) and PBA (synthesized according to ref. 30) were used as 100 mM stock in DMSO, cytD (Sigma) and oryzalin (Duchefa) as 100 mM stock in ethanol, and cycloheximide (Sigma) as 50 mM stock in water.

Whole-mount immunofluorescence analysis on root tips

Immunofluorescence analysis was carried out as described[27] or according to ref. 18 using an InsituPro machine (Intavis) for changing solutions. Rabbit polyclonal anti-PIN1 (ref. 17) was diluted at 1:200, mouse monoclonal anti-PM-ATPase at 1:500 and rabbit polyclonal anti-KNOLLE[27] at 1:4,000. Double labelling of KNOLLE PIN1 was done with polyclonal rat anti-KNOLLE serum. CY3- and fluorescein-isothiocyanate-conjugated secondary antibodies were from Dianova. We carried out confocal laser scanning microscopy with Leica microscopes.

Immunolocalization on cryosections and electron microscopy

Ultrastructure analysis of chemically fixed sections and immunogold labelling using silver-enhanced nanogold of ultrathin cryosections were carried out as described[29].

Received 3 July; accepted 9 August 2001.

1. Estelle, M. Polar auxin transport. New support for an old model. *Plant Cell* **10,** 1775–1778 (1998).
2. Berleth, T. & Sachs, T. Plant morphogenesis: long-distance coordination and local patterning. *Curr. Opin. Plant Biol.* **4,** 57–62 (2001).
3. Morris, D. A. Transmembrane auxin carrier systems—dynamic regulators of polar auxin transport. *Plant Growth Reg.* **32,** 161–172 (2000).
4. Palme, K. & Gälweiler, L. PIN-pointing the molecular basis of auxin transport. *Curr. Opin. Plant Biol.* **2,** 375–381 (1999).
5. Hadfi, K., Speth, V. & Neuhaus, G. Auxin-induced developmental patterns in *Brassica juncea* embryos. *Development* **125,** 879–887 (1998).
6. Mattsson, J., Sung, Z. R. & Berleth, T. Responses of plant vascular systems to auxin transport inhibition. *Development* **126,** 2979–2691 (1999).
7. Sabatini, S. *et al.* An auxin-dependent distal organizer of pattern and polarity in the *Arabidopsis* root. *Cell* **99,** 463–472 (1999).
8. Delbarre, A., Muller, P. & Guern, J. Short-lived and phosphorylated proteins contribute to carrier-mediated efflux, but not to influx, of auxin in suspension-cultured tobacco cells. *Plant Physiol.* **116,** 833–844 (1998).
9. Morris, D. A. & Robinson, J. S. Targeting of auxin carriers to the plasma membrane: differential effects of brefeldin A on the traffic of auxin uptake and efflux carriers. *Planta* **205,** 606–612 (1998).
10. Michalke, W., Katekar, G. F. & Geissler, A. E. Phytotropin-binding sites and auxin transport in *Cucurbita pepo*: evidence for two recognition sites. *Planta* **187,** 254–260 (1992).
11. Cox, D. N. & Muday, G. K. NPA binding activity is peripheral to the plasma membrane and is associated with the cytoskeleton. *Plant Cell* **6,** 1941–1953 (1994).
12. Bernasconi, P., Patel, B. C., Reagan, J. D. & Subramanian, M. V. The *N*-1-naphthylphthalamic acid-binding protein is an integral membrane protein. *Plant Physiol.* **111,** 427–432 (1996).
13. Fujita, H. & Syono, K. Genetic analysis of the effects of polar auxin transport inhibitors on root growth in *Arabidopsis thaliana*. *Plant Cell Physiol.* **37,** 1094–1101 (1996).
14. Garbers, C. *et al.* A mutation in protein phosphatase 2A regulatory subunit A affects auxin transport in *Arabidopsis*. *EMBO J.* **15,** 2115–2124 (1996).
15. Ruegger, M. *et al.* Reduced naphthylphthalamic acid binding in the *tir3* mutant of *Arabidopsis* is associated with a reduction in polar auxin transport and diverse morphological defects. *Plant Cell* **9,** 745–757 (1997).
16. Fujita, H. & Syono, K. *PIS1*, a negative regulator of the action of auxin transport inhibitors in *Arabidopsis thaliana*. *Plant J.* **12,** 583–595 (1997).
17. Gälweiler, L. *et al.* Regulation of polar auxin transport by AtPIN1 in *Arabidopsis* vascular tissue. *Science* **282,** 2226–2230 (1998).
18. Müller, A. *et al. AtPIN2* defines a locus of *Arabidopsis* for root gravitropism control. *EMBO J.* **17,** 6903–6911 (1998).
19. Steinmann, T. *et al.* Coordinated polar localization of auxin efflux carrier PIN1 by GNOM ARF GEF. *Science* **286,** 316–318 (1999).
20. Klausner, R. D., Donaldson, J. G. & Lippincott-Schwartz, J. Brefeldin A: insights into the control of membrane traffic and organelle structure. *J. Cell Biol.* **116,** 1071–1080 (1992).
21. Lippincott-Schwartz, J. *et al.* Microtubule-dependent retrograde transport of proteins into the ER in the presence of brefeldin A suggests an ER recycling pathway. *Cell* **60,** 821–836 (1990).
22. Wood, S. A., Park, J. E. & Brown, W. J. Brefeldin A causes a microtubule-mediated fusion of the trans-Golgi network and early endosomes. *Cell* **67,** 591–600 (1991).
23. Satiat-Jeunemaitre, B. & Hawes, C. Redistribution of a Golgi glycoprotein in plant cells treated with brefeldin A. *J. Cell Sci.* **103,** 1153–1156 (1992).
24. Satiat-Jeunemaitre, B. *et al.* Brefeldin A effects in plant and fungal cells: something new about vesicle trafficking? *J. Microsc.* **181,** 162–177 (1996).
25. Satiat-Jeunemaitre, B., Steele, C. & Hawes, C. Golgi-membrane dynamics are cytoskeleton dependent: a study on Golgi stack movement induced by brefeldin A. *Protoplasma* **191,** 21–33 (1996).
26. Mathur, J., Spielhofer, P., Kost, B. & Chua, N.-H. The actin cytoskeleton is required to elaborate and maintain spatial patterning during trichome cell morphogenesis in *Arabidopsis thaliana*. *Development* **126,** 5559–5568 (1999).
27. Lauber, M. H. *et al.* The *Arabidopsis* KNOLLE protein is a cytokinesis-specific syntaxin. *J. Cell Biol.* **139,** 1485–1493 (1997).
28. Völker, A., Stierhof, Y.-D. & Jürgens, G. Cell cycle-independent expression of the *Arabidopsis* cytokinesis-specific syntaxin KNOLLE results in mistargeting to the plasma membrane and is not sufficient for cytokinesis. *J. Cell Sci.* (in the press).
29. Hager, A. *et al.* Auxin induces exocytosis and the rapid synthesis of a high-turnover pool of plasma-membrane H^+-ATPase. *Planta* **185,** 527–537 (1991).
30. Kategar, G. F. & Geissler, A. E. Auxin transport inhibitors. *Plant Physiol.* **60,** 826–829 (1977).

Acknowledgements

We thank A. Vieten and S. Barth for technical assistance; L. Gälweiler, W. Michalke and K. Roberts for kind gifts of antibodies; S. M. Li for MS/NMR analysis; and M. Godde, M. Heese, T. Hamann, T. Pacher and K. Schrick for helpful comments and critical reading of the manuscript. J. F. was a recipient of a *Deutscher Akademischer* Austauschdienst fellowship. This work was supported by Deutsche Forschungsgemeinschaft (DFG), Schwerpunktprogramm'Molekulare Analyse der Phytohormonwirkung', European Communities Biotechnology Programme and INCO Copernicus Programme (K.P.), and DFG, Sonderforschungsbereich 'Mechanismen des Zellverhaltens bei Eukaryoten' (G. J.).

Correspondence and requests for materials should be addressed to G.J. (e-mail: gerd.juergens@zmbp.uni-tuebingen.de).

Voltage-induced membrane movement

Ping-Cheng Zhang, Asbed M. Keleshian & Frederick Sachs

HHMI Center for Single Molecule Biophysics, State University of New York at Buffalo, Buffalo, New York 14214, USA

Thermodynamics predicts that transmembrane voltage modulates membrane tension[1] and that this will cause movement. The magnitude and polarity of movement is governed by cell stiffness and surface potentials. Here we confirm these predictions using the atomic force microscope to dynamically follow the movement of voltage-clamped HEK293 cells[2] in different ionic-strength solutions. In normal saline, depolarization caused an outward movement, and at low ionic strength an inward movement. The amplitude was proportional to voltage (about 1 nm per 100 mV) and increased with indentation depth. A simple physical model of the membrane and tip provided an estimate of the external and internal surface charge densities (-5×10^{-3} C m^{-2} and -18×10^{-3} C m^{-2}, respectively). Salicylate (a negative amphiphile[3]) inhibited electromotility by increasing the external charge density by -15×10^{-3} C m^{-2}. As salicylate blocks electromotility in cochlear outer hair cells at the same concentration[4,5], the role of prestin as a motor protein[6] may need to be reassessed.

The Lippman[1] equation relates interfacial tension to electrostatic potential. The physical basis for this thermodynamic relationship stems from properties of the double layer adjacent to polarizable interfaces. This region contains excess mobile charges that are attracted to the fixed structural charges or are supplied by external voltage sources. These mobile charges repel each other laterally, creating a local pressure and changing the net surface tension. In lipid monolayers, changes in ionic strength alter the surface pressure (tension)[7]. Membrane movements correlated with action potentials have been observed in crab nerve as well as squid giant axon[8]. In a bilayer membrane with two interfaces, a difference in tension between the interfaces can cause changes in curvature, an effect also known as converse flexoelectricity. Both flexoelectricity (current generation from bending) and its converse have been demonstrated in lipid bilayers[9] and cell membranes[10].

When an atomic force microscope (AFM) tip indents a membrane, changes in membrane tension will move the cantilever[2]. We have measured these displacements in real time using voltage-clamped HEK293 cells (Fig. 1a). A simple model that applies the Lippmann equation to both interfaces explains the observed movement over a wide range of surface potentials and applied voltage. As the Lippmann equation is derived from thermodynamic principles, the basic model should apply to all membranes.

As can be seen from Fig. 1b, in normal saline hyperpolarizing pulses cause the cantilever to move towards the cell interior, whereas depolarization reverses the movement. At low ionic strength (isosmotic 288 mM sucrose, ionic strength 20 μM measured by conductivity) the potential dependence inverts. The time-dependent changes seen in Fig. 1b may result from cytoskeletal relaxation or lipid flip-flop (the movement of lipid molecules between the internal and external monolayers), and are the subject of an ongoing study. The peak displacement is linear with voltage (Fig. 1c) and increases with the mean indentation force (Fig. 1d). The peak displacement as a function of the bath ionic strength is shown in Fig. 2a for both hyperpolarizing and depolarizing pulses (± 100 mV, from a holding potential of −60 mV). Note the reversal of movement at about 10 mM.

We modelled the system by applying the Lippmann equation at both interfaces (assumed independent[11]) and treating the bilayer as an incompressible capacitor. Whereas the mean force on an indent-